8. Craciun, R. *et al.* A novel method for preparing anode cermets for solid oxide fuel cells. *J. Electrochem. Soc.* **146**, 4019–4022 (1999).

9. Trovarelli, A. Catalytic properties of ceria and CeO₂ -containing materials. *Catal. Rev. Sci. Eng.* **38**, 439–520 (1996).

10. Marina, O. A. & Mogensen, M. High-temperature conversion of methane on a composite gadolinia-doped ceria-gold electrode. *Appl. Catal. A* **189**, 117–126 (1999).

11. Christensen, H., Dinesen, J., Engel, H. H. & Hansen, K. K. *Electrochemical Reactor For Exhaust Gas Purification* 1–5 (Society of Automotive Engineers paper no. 1999-01-0472, Warrendale, Philadelphia, 1999).

12. Yamanaka, I. & Otsuka, K. Catalysis of Sm⁺³ for the oxidation of alkanes with O₂ in the liquid phase. *J. Mol. Catal. A* **95**, 115–120 (1995).

....

Single crystals of an ionic anthracene aggregate with a triplet ground state

H. Bock*, **K. Gharagozloo-Hubmann***, **M. Sievert***, **T. Prisner***
& Z. Havlas†

* *Department of Chemistry, Johann Wolfgang Goethe University, Marie Curie Strasse 11, D-60439 Frankfurt am Main, Germany*
† *Institute of Organic Chemistry and Biochemistry of the Czech Academy of Sciences, Flemingovo Nam 2, CZ-16610 Prague, Czech Republic*

....

Crystalline supramolecular aggregates consisting of charged organic molecules, held together through metal-cluster-mediated Coulomb interactions, have attracted interest owing to their unusual structural, chemical and electronic properties[1–3]. Aggregates containing metal cation clusters 'wrapped' by lipophilic molecular anions have, for example, been shown[4,5] to be kinetically stable and soluble in nonpolar liquids such as saturated hydrocarbons. The formation of supramolecular aggregates can even be exploited to generate aromatic hydrocarbons that carry four negative charges and crystallize in the form of organic poly(metal cation) clusters[6,7] or helical polymers[8]. Here we report the anaerobic crystallization of an ionic organic aggregate—a contact ion septuple consisting of a fourfold negatively charged 'tripledecker' of three anthracene molecules bridged by four solvated potassium cations. Its electronic ground state is shown experimentally, using temperature-dependent electron paramagnetic resonance spectroscopy, to be a triplet. Although the spins in this biradical ionic solid are separated by a considerable distance, density functional theory calculations[9] indicate that the triplet ground state is 84 kJ mol⁻¹ more stable than the first excited singlet state. We expect that the successful crystallization of the ionic solid we report here, and that of a covalent organic compound with a triplet ground state[10] at room temperature, will

stimulate further attempts to develop new triplet-ground-state materials for practical use.

Molecular anions M^{n-} and their countercations Met^+_{solv} (where Met is the alkali metal) crystallize from aprotic solvents either as solvent-separated $[M^{n-}][Met^+_{solv}]_n$ or as solvent-shared $[M^{n-}Met^+_n]_{solv}$ ion pairs[11,12]. They are formed in a multidimensional network of solution equilibria[13] involving electron transfer and contact ion pair formation as well as aggregation, and are often dominated by cation solvation[14]; such solvation is known to control numerous chemical reactions, including geochemical and biochemical reactions. For instance, if the π-hydrocarbon anthracene is reduced in ether or alkylamine solutions at alkali-metal surfaces [Met]$_x$, slight modifications of the conditions lead to various reduction products which can be structurally characterized in single crystals[15,16] (Fig. 1).

The manifold of possible anthracene anion salt structures (Fig. 1) ranges from the solvent-separated sodium salt of the bare anthracene radical anion[15] (Fig. 1a), via the double η^6-half-sandwichs of two [Li⁺TMEDA] ligands on both faces of the anthracene dianion[16] (Fig. 1b), to the ion quadruple of two anthracene radical anions connected by a $[K_2^+THF_3]^{+2}$ bridge (Fig. 1c) (see Methods), and stimulated attempts to crystallize even larger aggregates. (THF, tetrahydrofuran; TMEDA, tetramethylethylenediamine.)

Low-gradient crystallization by diffusion of n-hexane from an added layer into the blue THF solution of anthracene that is reduced at a potassium metal mirror yields—after three days standing at room temperature—black needles with a violet lustre (see Methods). On further standing of the decanted solution, another batch of black needles is collected. X-ray structure analysis proves the first crystal fraction to be the title compound (that is, the contact ion septuple $[(anthracene)_3^{4-}(K_2^+THF_3)_2^{+2}]_1$ (Fig. 2), whereas the second batch contains the smaller aggregate $[(anthracene)_2^{2-}(K_2^+THF_3)^{+2}]_1$ (Fig. 1c). This suggests that the smaller compound might act as a 'seed', from which the crystal of the three-layered anthracene tetraanion (Fig. 2) might grow.

The crystal structure analysis of the anthracene potassium septuple (Fig. 2) reveals a hitherto unknown type of hydrocarbon aggregate: in the centrosymmetric double sandwich, the planar anthracene anions exhibit centroid/centroid distances of 565 pm and are tilted by interplanar angles of +54° and −54°. The four K⁺ centres (with a total coordination number of 14) are each η^6-connected to the peripheral six-membered rings with contacts K⁺···C$^{\delta-}$ of 312–322 pm length to the outer anthracene ligands, and of 290–335 pm to the central anthracene; the perpendicular distances K⁺···ring amount to 289 and 275 pm. (C$^{\delta-}$ indicates partial changes at the individual centres.) The K⁺ centres are 431 pm apart, and each one exhibits two contacts K⁺···O to the O centres of two THF solvate ligands of lengths 265 and 285 pm. The planar anthracene anion rings are distorted differently: relative to the neutral molecule, the bonds C1–C2 are shortened by 4 pm and C2–C3 are elongated by 2 pm for the outer ligands, or shortened by 5 pm and elongated by 4 pm for the central dianionic bridge. This structural diversity is already known from published anthracene anion structures[15,16] (Fig. 1), and suggests that the outer ligands are
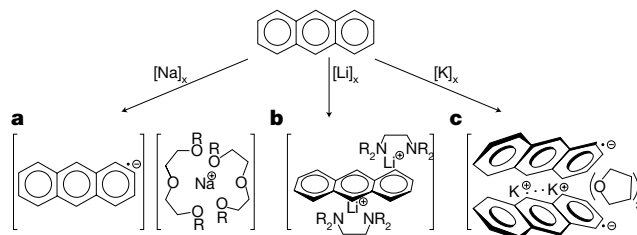
Figure 1 Selected examples of anthracene anion salts. **a**, Anthracene radical anion-sodium bis(triglyme) (ref. 15); **b**, anthracene dianion-dilithium-bis(TMEDA) (ref. 16); **c**, $[(anthracene)_2^{2-}(K_2^+ THF_3)^{+2}]_1$ (see Methods).
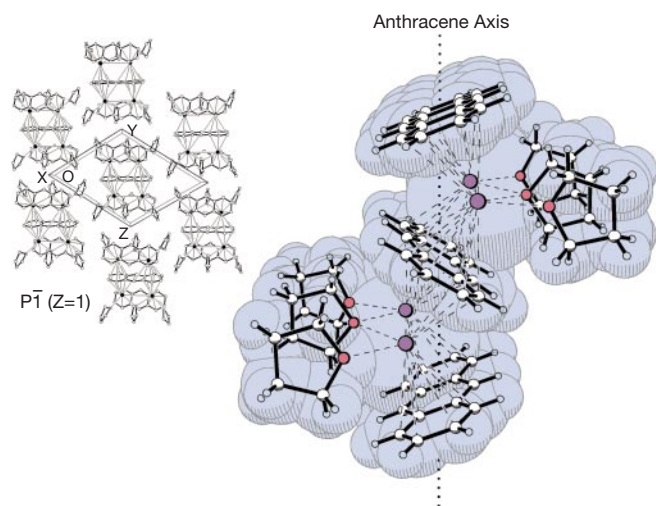
267

Figure 2 Single-crystal structure of [(anthracene$^{\bullet-}$) (K$_2^+$THF$_3$)$^{+2}$ anthracene^{2-} (K$_2^+$THF$_3$)$^{+2}$ (anthracene$^{\bullet-}$)] at 150 K. Shown is the unit cell P$\bar{1}$ ($Z = 1$) with adjacent aggregates, and its space-filled as well as skeletal structures (colour code: C and H, white; O, red; K violet). In the text, this compound is referred to as [(anthracene)$_3^{4\bullet}$(K$_2^+$THF$_3$)$_2$]$_1$, for brevity; the longer formula is used here to aid comparison with the space-filling structure.

Figure 3 Rabi oscillations of the EPR signal of a single crystal of [(anthracene)$_3^{4-}$(K$_2^+$THF$_3$)$_2^{+2}$]$_1$. The oscillation frequencies have been calibrated by two standard samples; one with a spin-state $S = 1/2$, the other with a spin-state $S = 5/2$ (see Methods for details). All measurements were performed under identical conditions (same Q value of microwave cavity, microwave excitation power, sample size and temperature). The observed Rabi frequencies were 7 MHz for the $S = 1/2$ standard, 9.5 MHz for the anthracene crystals, and 24 MHz for the $S = 5/2$ standard. These measurements show clearly that the spin state of the observed signal corresponds to a triplet state (see Methods for rationale).

anthracene radical anions, whereas the central anthracene unit should rather be a dianion. The structure that we determined for the anthracene potassium quintuple (Fig. 1c), the potential 'seed' intermediate that was crystallized separately from the same solution (see Methods), shows many similarities: the interplanar tilting angle between the two anthracene radical anions amounts to 57° and their centroid/centroid distance to 490 pm.

Starting from the crystal structure coordinates, we performed unrestricted density functional theory (DFT) UB3LYP/6-31G* calculations for both the 154-atom contact ion septuple (Fig. 2) and the 89-atom contact ion quintuple (Fig. 1c) in both their singlet and their triplet states (see Methods). Unexpectedly, in both cases the triplet states were predicted to be more stable, by 84 kJ mol^{-1} for [(anthracene)$_3^{4-}$(K$_2^+$THF$_3$)$_2^{+2}$]$_1$ (Fig. 2 and Table 1) and by 13 kJ mol^{-1} for [(anthracene)$_2^{2-}$(K$^+$THF$_3$)$^{+2}$]$_1$ (Fig. 1c).

The DFT/natural bond orbital charges that we calculated (Table 1) differ only slightly for the singlet and the triplet state (Fig. 1), but the spin is predicted to be located almost exclusively in the two outer anthracene radical anion ligands, the centroids of which are 1,030 pm apart, on both sides of the central anthracene dianion mediating the spin–spin interaction.

Different spin states S can be distinguished with pulsed electron paramagnetic resonance (EPR) measurement by their distinct Rabi oscillation frequency under resonant coherent microwave excitation[17]. Theoretically, the Rabi frequency scales with $\sqrt{S(S+1) - m_S(m_S + 1)}$ for a transition from m_S to m_{S+1}.

We compared the observed Rabi frequency for the anthracene crystals with standard calibration samples (see Fig. 3 and Methods), and demonstrated clearly that the observed signal from the crystals corresponds to a triplet state ($S = 1$). For such a triplet spin state, a typical dipolar splitting of the EPR line by $(D/r^3)(3\cos^2\theta - 1)$ (where D is the dipolar coupling constant, r is the spin–spin distance, and q is the angle between dipolar vector and external magnetic field) would be expected to be directly observable in the spectrum. Instead, only a narrow homogeneous line (line-width $\Delta\omega_{1/2} = 2/T_2 = 2/T_1$ with T_1 longitudinal and T_2 transversal relaxation times) without any dipolar and hyperfine contribution was observed. The reason that the dipolar coupling of the triplet spin
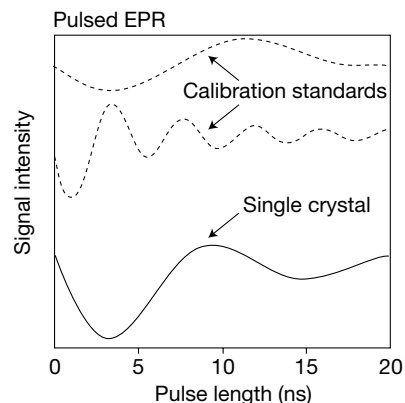
cannot be observed in the continuous-wave EPR spectra might be due to a strong exchange coupling of the triplet states in the crystal, which would narrow the EPR signal to a homogeneous line.

The crystallization of the three-layered trianthracene tetraanion potassium salt, as well as its predicted and proven triplet ground state at room temperature, are of general importance both for multielectron reduction processes of molecules in solution and for the design of new biradical ionic solids. We conclude that the sterically limited solvation by THF, known for Na$^+$ countercations[14], favours the self-aggregation within the solvent-dependent equilibria network of electron transfer and contact ion formation[13]. From this solution both the anthracene trimer (Fig. 2) as well as the dimer biradical (Fig. 1c) crystallize selectively. The trianthracene contact ion septuple described here seems to be the first crystalline organic ionic material for which a triplet biradical ground state has been calculated and confirmed by EPR measurement. The structure of a neutral triplet biradical, tris(3,5-di(t-butyl)-4-oxophenylene) methane at room temperature, has been reported before[10].

We consider that the crystallization and structural characterization of covalent as well as ionic organic compounds with a triplet ground state should stimulate further investigations. In particular, our work suggests that the synthesis of air-stable biradicals with lipophilically shielding paramagnetic organometallic ligands on both ends of a suitable spin propagating transductor seems to be feasible. Also, referring especially to the exchange coupling between adjacent aggregates within the crystal lattice, the exploration of the physical properties as well as the potential technical applications of new triplet-ground-state materials could be rewarding. □

Methods

Preparation and crystal growth of compounds

From 140 mg (7.6 mmol) potassium, a metal mirror is generated on the wall of a dried Schlenk trap by gentle heating at 10^{-5} mbar. Addition of 310 mg (1.7 mmol) of anthracene in 10 ml aprotic tetrahydrofuran (THF) ($c_{H+} < 1$ p.p.m.) produces a blue solution, which after 1 day of standing at room temperature is covered with a layer of 24 ml n-hexane. After another 3 days, black crystals with a violet lustre of [(anthracene)$_3^{4\bullet}$(K$_2^+$THF$_3$)$_2^{2+}$]$_1$ (Fig. 2) are collected from the trap wall near the phase border line. Keeping the solution for another 7 days at room temperature yields black crystals with a violet lustre of [(anthracene)$_2^{2-}$(K$_2^+$THF$_3$)$^{+2}$]$_1$THF] (Fig. 1c).

X-ray structure analyses

[(anthracene)$_3^{4-}$(K$_2^+$THF$_3$)$_2^{2+}$]$_1$ (Fig. 2). Space group P$\bar{1}$, $a = 9.388(2)$, $b = 13.265(2)$, $c = 14.192(2)$ Å, $\alpha = 62.876(8)$, $\beta = 85.20(1)$, $\gamma = 70.47(1)°$, $V = 1477.5(5)$ Å^3, $Z = 1$, $\rho = 1.263$ g cm^{-3}, $\mu = 0.35$ mm^{-1}, $F(000) = 598$, crystal size $= 0.4 \times 0.35 \times 0.35$ mm; crystals were removed from the trap wall after 4 days under argon, immediately immersed in perfluor-polyether oil and mounted under a flow of nitrogen cooled to 150 K on a Siemens P4 diffractometer (Mo Kα, graphite monochromator). A total of 6,211 reflections (2.31 $< \Theta <$ 26.27°) were collected, of which 4,911 unique reflections ($R_{int} = 0.0308$) were used. The structure was solved using the program SHELXS-93 and refined (343 parameters) using the program SHELXS-93 to $R = 0.0434$ for 3,941 reflections with $I > 2\sigma(I)$ (both programs from G. M. Sheldrick, Univ. Göttingen, 1993).

[(anthracene)$_2^{2-}$(K$_2^+$THF$_3$)$^{+2}$]$_1$ (Fig. 1c). Space group C2/c, $a = 14.186(3)$, $b = 10.633(2)$, $c = 23.382(4)$ Å, $\beta = 103.78(1)°$, $V = 3425.4(11)$ Å^3, $Z = 4$, $\rho = 1.262$ g cm^{-3}, $\mu = 0.314$ mm^{-1}, $F(000) = 1,384$, crystal size $= 0.25 \times 0.62 \times 0.84$ mm; crystals were removed from the trap wall after 11 days under argon, immediately immersed in perfluor-polyether oil and mounted under a flow of nitrogen cooled to 150 K on a Siemens P4 diffractometer (Mo Kα, graphite monochromator). A total of 3,783 reflections (2.42 $< \Theta <$ 25°) were collected, of which 2,995 unique reflections ($R_{int} = 0.0337$) were used. The structure was solved using the program SHELXS-93 and refined (203 parameters) using the program SHELXS-93 to $R = 0.0507$ for 1,801 reflections with $I > 2\sigma(I)$ (both programs from G. M. Sheldrick, Univ. Göttingen, 1993). The β-carbon centres of the THF ligand in the middle position are disordered over two positions with site occupation factors of 0.49 and 0.51.

Unrestricted density functional theory calculations

For both the rather large aggregates [(anthracene)$_3^{4-}$(K$_2^+$THF$_3$)$_2^{2+}$] and [(anthracene)$_2^{2-}$(K$_2^+$THF$_3$)$^{+2}$], the singlet- and triplet-state computations have been performed at the UB3LYP/6-31G* level, using the NEC SX4 supercomputer of the Höchstleistungs-Rechenzentrum Stuttgart, Germany using the Gaussian 94 program package[9]. The singlet-state calculations were started from the broken symmetry orbital. The total energies of the triplet states are calculated to be −5384.72797 a.u. and −2976.24778 a.u. The charge and spin distributions were obtained by natural bond orbital analysis after enlarging the capacity of the corresponding program module.

EPR measurements

Pulsed and continuous-wave EPR measurements were performed with a Bruker E580 ELEXIS X-band spectrometer. Single crystals (4 × 0.35 × 0.35 mm) were sealed in 3-mm-diameter X-band quartz EPR capillaries under argon in n-hexane solution. The single crystals give rise to a narrow homogeneous EPR line, with a linewidth of 1.9 G and a g value close to 2, typical for a π-delocalized organic radical. No dipolar splitting of the signal could be observed in the temperature range 10–290 K. The Rabi oscillation behaviour of the signal[17] of these crystals have been compared with a spin-state $S = 1/2$ radical salt of perylene ((perylenyl)$_2$(AsF$_6$)$_{0.75}$(PF$_6$)$_{0.35}$·0.85 CH$_2$Cl$_2$) and a spin-state $S = 5/2$ MnO sample (only the central $m_S = -1/2$ to +1/2 transition observed) under identical conditions (same Q value of microwave cavity, microwave excitation power, sample size and temperature). The theoretical predicted ratio of the oscillation frequencies are $1 : \sqrt{2} : 3$ for a $S = 1/2$, a $S = 1$ and the $m_S = -1/2$ to +1/2 transition of a $S = 5/2$ spin state. The observed Rabi frequencies were 7 MHz for $S = 1/2$, 9.5 MHz for the anthracene crystals, and 24 MHz for the MnO sample. Therefore these measurements clearly showed that the spin state of the observed signal corresponds to a triplet state. The temperature dependence (10–290 K) of the EPR signal as well as the absolute signal intensity exclude an assignment of the signal to a low-lying excited triplet state or to impurities or defects. Taken together, these measurements prove that the ground state of this compound is indeed a triplet spin state.

1. Lehn, J. M. Supramolecular Chemistry, Concepts and Perspectives (VCH, Weinheim, 1995).
2. Müller, A., Reuter, H. & Dillingers, S. Supramolecular inorganic chemistry: small guests in small and large hosts. Angew. Chem. Int. Edn Engl. 34, 2326–2361 (1995).
3. Müller, A., Shah, S. Q. N., Bögge, H. & Schmidtmann, M. Molecular growth from a Mo$_{176}$ to a Mo$_{248}$ cluster. Nature 397, 48–50 (1999).
4. Bock, H., Lehn, J. M., Pauls, J., Holl, S. & Krenzel, V. Sodium salts of the bipyridine dianion polymer[(bpy)$^{2-}$[Na$^+$(dme)]$_2$]$_x$ cluster [(Na$_8$O)$^{6+}$Na$_6^+$(bpy)$_6^{2-}$ (tmeda)$_6$], and monomer [(bpy)$^{2-}$[Na$^+$(pmdta)]$_2$]. Angew. Chem. Int. Edn. Engl. 38, 952–955 (1999).
5. Bock, H. et al. The lipophilically wrapped polyion aggregate {[Ba$_6$Li$_3$O$_2$]$^{11+}$[$^-$OC(CH$_3$)$_3$]$_{11}$ (OC$_4$H$_8$)$_3$}, a face-sharing (octahedron + prismane) Ba$_6$Li$_3$O$_2$ polyhedron in a hydrocarbon ellipsoid: preparation, single crystal structure analysis, and density functional calculations. Angew. Chem. Int. Edn. Engl. 34, 1353–1355 (1995).
6. Bock, H., Gharagozloo-Hubmann, K., Näther, C., Nagel, N. & Havlas, Z. [{Na$^+$(thf)}$_4$(rubrene)$^{4-}$] crystallisation and structure determination of a contact ion quintuple for the first π-hydrocarbon-tetraanion. Angew. Chem. Int. Edn Engl. 35, 631–633 (1996).
7. Sekiguchi, A., Matsuo, T. & Kabuto, C. Synthesis and characterisation of the tetralithium salt of an octasilyl-substituted trimethylencyclopentadien-tetraanion. Angew. Chem. Int. Edn Engl. 36, 2462–2464 (1997).
8. Bock, H., Gharagozloo-Hubmann, K., Sievert, M. & Havlas, Z. Synthesis, crystal growth and structure determination of [(6,13'-Dipentacene$^{\ominus 4}$)(K$^{\oplus}$DME)$_4$]$_\infty$: a twin-strand polymer helix. Angew. Chem. Int. Edn Engl. (submitted).
9. Havlas, Z. & Bock, H. Bare molecular anions of the saturated hydrocarbons: density functional charge and spin distribution based on their single crystal structures. Collect. Czech. Chem. Commun. 63, 1245–1263 (1998).
10. Bock, H., John, A., Havlas, Z. & Bats, J. W. The triplet biradical tris(3,5-di(tert-butyl)4-oxophenyl-
11. lene)methane: crystal structure, spin and charge distribution. Angew. Chem. Int. Edn Engl. 32, 416–418 (1993).
11. Bock, H., Näther, C., Ruppert, K. & Havlas, Z. Tetraphenylbutadiene disodium dimethoxyethene: solvent-shared and solvent-separated ion triples within a single crystal. J. Am. Chem. Soc. 114, 6907–6908 (1992).
12. Bock, H., Näther, C., Ruppert, K. & Havlas, Z. Competing Na$^{\oplus}$ solvation: ether-shared and ether-separated triple ions of perylene dianion. J. Am. Chem. Soc. 117, 3869–3870 (1995).
13. Bock, H. et al. Distorted molecules: perturbation design, preparation and structures. Angew. Chem. Int. Edn Engl. 31, 550–581 (1992).
14. Bock, H., Näther, C., Havlas, Z., John, A. & Arad, C. Ether-solvated sodium ions in salts containing π-hydrocarbon anions: crystallisation, structures and semiempirical solvation energies. Angew. Chem. Int. Edn Engl. 33, 875–878 (1994).
15. Bock, H., Arad, C., Näther, C. & Havlas, Z. The structure of solvent-separated naphthalene and anthracene radical anions. J. Chem. Soc. Chem. Commune. 2393–2394 (1995).
16. Rhine, W. E., Davis, J. & Stucky, G. Anthracene dianion dilithium bis(TMEDA). J. Am. Chem. Soc. 97, 2079–2085 (1975).
17. Stoll, S., Jeschke, G., Willer, M. & Schweiger, A. Nutation-frequency correlated EPR spectroscopy: the PEANUT experiment. J. Magn. Reson. 130, 86–96 (1998).

....

Seismic hazard in the Marmara Sea region following the 17 August 1999 Izmit earthquake

Aurélia Hubert-Ferrari*, Aykut Barka†, Eric Jacques‡, Süleyman S. Nalbant§, Bertrand Meyer‖, Rolando Armijo‖, Paul Tapponnier‖ & Geoffrey C. P. King‖

* Department of Geosciences, Princeton University, Princeton, New Jersey 08544, USA
† ITU, Maden Fakultesi, Jeoloji Bolumu, Ayazaga, Istanbul, Turkey
‡ Observatoire des Sciences de la Terre de Strasbourg (UMS 830 of CNRS), Strasbourg, France
§ Geophysics Department, Engineering Faculty, Istanbul University, Istanbul, Turkey
‖ Laboratoire de Tectonique et Mécanique de la Lithosphère (UMR 7578 of CNRS), Institut de Physique du Globe, Paris

....

On 17 August 1999, a destructive magnitude 7.4 earthquake occurred 100 km east of Istanbul, near the city of Izmit, on the North Anatolian fault. This 1,600-km-long plate boundary[1,2] slips at an average rate of 2–3 cm yr^{-1} (refs 3–5), and historically has been the site of many devastating earthquakes[6,7]. This century alone it has ruptured over 900 km of its length[6]. Models of earthquake-induced stress change[8] combined with active fault maps[9] had been used to forecast that the epicentral area of the 1999 Izmit event was indeed a likely location for the occurrence of a large earthquake[9,10]. Here we show that the 1999 event itself significantly modifies the stress distribution resulting from pre-vious fault interactions[9,10]. Our new stress models take into account all events in the region with magnitudes greater than 6 having occurred since 1700 (ref. 7) as well as secular interseismic stress change, constrained by GPS data[11]. These models provide a consistent picture of the long term spatio–temporal behaviour of the North Anatolian fault and indicate that two events of magni-